PALEONTOLOGY

Decoupled taxonomic and ecological recoveries from the Permo-Triassic extinction

Haijun Song[1,2]*, Paul B. Wignall[2], Alexander M. Dunhill[2]

Copyright © 2018 The Authors, some rights reserved; exclusive licensee American Association for the Advancement of Science. No claim to original U.S. Government Works. Distributed under a Creative Commons Attribution NonCommercial License 4.0 (CC BY-NC).

The Permian-Triassic mass extinction was the worst crisis faced by life; it killed >90% of marine species in less than 0.1 million years (Ma). However, knowledge of its macroecological impact over prolonged time scales is limited. We show that marine ecosystems dominated by non-motile animals shifted to ones dominated by nektonic groups after the extinction. In Triassic oceans, animals at high trophic levels recovered faster than those at lower levels. The top-down rebuilding of marine ecosystems was still underway in the latest Triassic, ~50 Ma after the extinction, and contrasts with the ~5-Ma recovery required for taxonomic diversity. The decoupling between taxonomic and ecological recoveries suggests that a process of vacant niche filling before reaching the maximum environmental carrying capacity is independent of ecosystem structure building.

INTRODUCTION

The Permian-Triassic (P-Tr) mass extinction of 252 million years (Ma) ago caused a transformation among marine communities from the Paleozoic evolutionary fauna to the modern evolutionary fauna (*1*), although there was a prolonged delay of recovery in the Early Triassic (*2*). Biodiversity data, compiled from global fossil databases and case studies, provide much detail on the magnitude and duration of the extinction (*3*–*5*), but knowledge of the associated ecosystem changes remains limited (*6*). It is generally thought that marine ecosystems took several million years to recover as survivors and that new taxa filled vacant ecospace (*7*), with recovery occurring in a stepwise manner from bottom to top trophic levels (*8*). In contradiction to this view, the discovery of diverse predators in Early Triassic oceans such as conodonts, ammonoids, and bony fishes suggests rapid recovery of pelagic predators (*9*–*11*). In addition, no significant loss of global functional diversity in benthic marine ecosystems was observed across the extinction, but there is an apparent lack of representation of several functional groups during the extinction interval as a result of either mass rarity (skeleton crew hypothesis) or lack of sampling, suggesting that ecological changes during this critical time are more complex than previously thought (*12*). To test the timing and pattern of ecosystem succession during and after the P-Tr extinction for the duration of the entire Triassic, we have analyzed the changing diversity among three functional groups (non-motile, motile, and nektonic animals; see Fig. 1) based on a new global fossil database compiled from the Paleobiology Database and published literatures (external database S1).

RESULTS AND DISCUSSION

Taxonomic recovery

Our new database includes occurrences of marine genera from the Late Permian (Changhsingian, 254.1 Ma ago) to the Late Triassic (Rhaetian, 201.3 Ma ago). A total of 51,055 occurrences derived from 1679 literature sources were collected to a substage- or stage-level resolution (table S1). An occurrence is defined as the presence of a given genus at a particular stratigraphic unit or site. Multiple occurrences of the same genus in a single collection were treated as a single occurrence. The subsampled diversity curve (Fig. 2A) shows key features of older curves (*1*, *3*), such as the significant diversity loss during the P-Tr extinction and delayed recovery. However, higher temporal resolution also reveals features that are not apparent in earlier curves, such as a pause of diversification in the middle Carnian, which is likely the result of the Carnian Pluvial Event (*13*). Following the P-Tr mass extinction, marine generic diversity finally attained pre-extinction levels in the early Anisian ~5 Ma later. This recovery coincides with clear evidence for environmental amelioration, especially ocean reoxygenation and climate cooling (*14*, *15*). The sampling-standardized curve shows a logistic increase in taxonomic diversity during the Triassic (see also Fig. 2B), supporting an equilibrium model similar to the Paleozoic plateau in marine invertebrate diversity (*1*, *16*) and suggesting that generic diversity appears to have reached the environmental carrying capacity. The biota of the Middle Triassic differs from Late Triassic biota in composition, but not in richness (Fig. 2).

Ecological recovery

To investigate macroecological changes, we assigned animals to three functional groups depending on their motile abilities (i.e.,

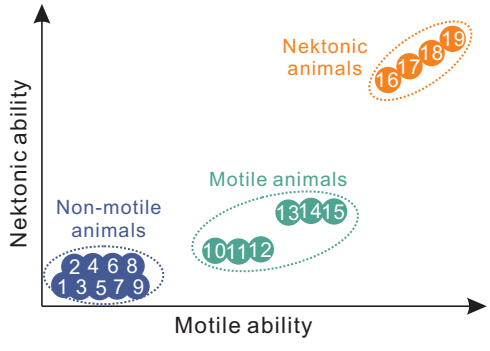

Fig. 1. Conceptual plot showing marine animals assigned to the three groups based on motile and nektonic abilities. 1, corals; 2, sponges; 3, brachiopods; 4, bryozoans; 5, pelmatazoan echinoderms; 6, foraminifers; 7, epifaunal bivalves; 8, radiolarians; 9, hydrozoans; 10, eleutherozoan echinoderms; 11, infaunal bivalves; 12, gastropods; 13, annelids; 14, ostracods; 15, non-ostracod crustaceans; 16, cephalopods; 17, conodonts; 18, fishes; 19, marine reptiles.

[1]State Key Laboratory of Biogeology and Environmental Geology, School of Earth Science, China University of Geosciences, Wuhan 430074, China. [2]School of Earth and Environment, University of Leeds, Leeds LS2 9JT, UK.
*Corresponding author. Email: haijun.song@aliyun.com

Downloaded from http://advances.sciencemag.org/ on September 24, 2020

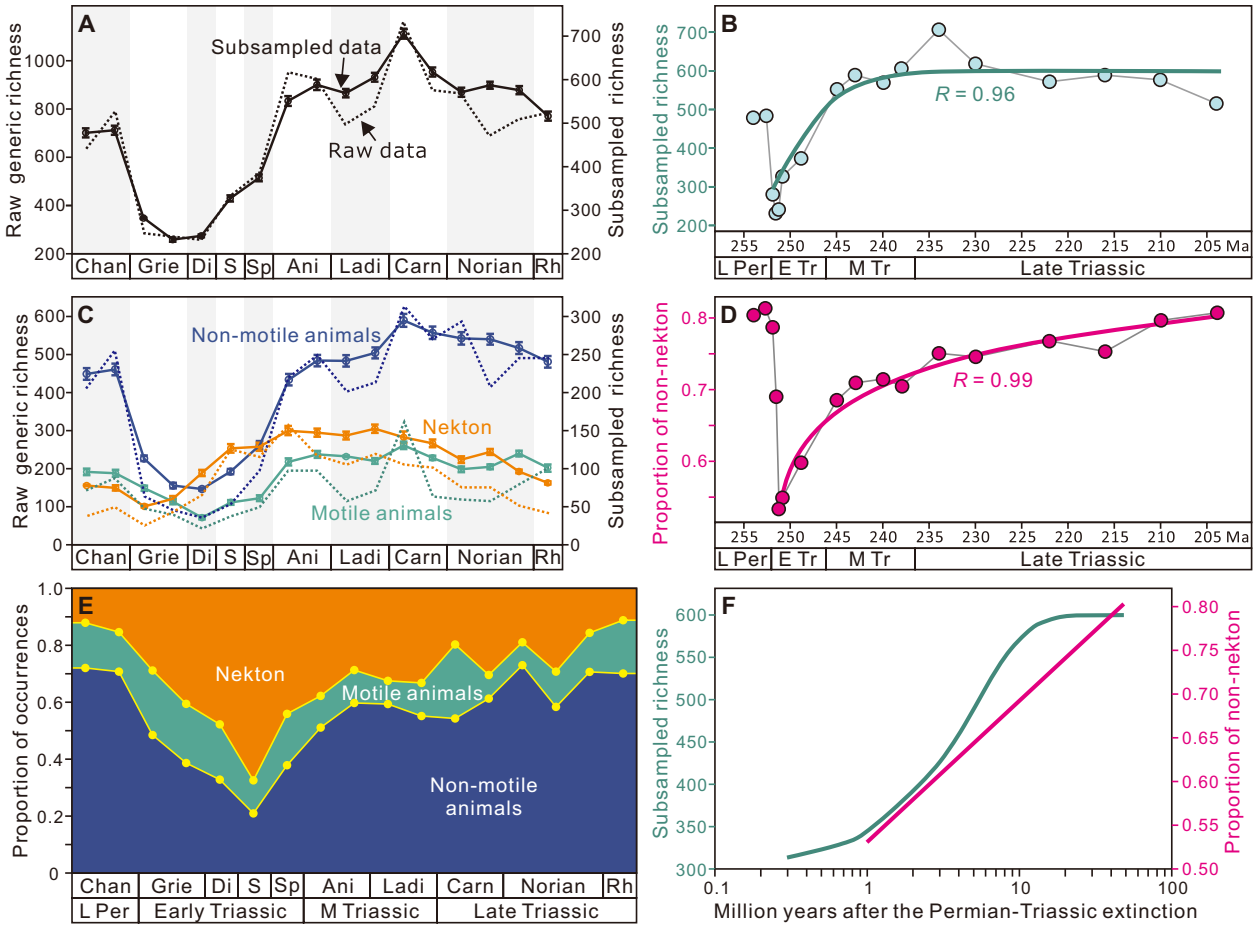

Fig. 2. Generic diversity and occurrences in time bins during the Late Permian and Triassic. (**A**) Counts of all marine genera in the full data set (dash line) and estimated counts using the subsampled data (solid line; fig. S1). Data are standardized by repeatedly subsampling from a randomly generated set until a quota of 1400 occurrences has been recovered in each bin. Vertical lines show the 95% confidence intervals. (**B**) Subsampled generic richness in time bins. The data are the same subsampled generic richness as shown in (A) but in different time scaling. Green curve shows a logistic increase ($R = 0.96$, $P \ll 0.001$) from Dienerian to Rhaetian. (**C**) Counts of marine genera in the full data set (dash lines) and using the subsampled data (solid lines). The subsampled quotas are 510, 184, and 330 for non-motile, motile, and nektonic groups, respectively. (**D**) Proportion of non-nektonic animals based on subsampled data in (C). Magenta curve shows a logarithmic increase ($R = 0.99$, $P \ll 0.001$) from Dienerian to Rhaetian. (**E**) Proportion of marine generic occurrences among non-motile, motile, and nektonic groups. (**F**) Changes of generic richness and proportion in a logarithmic coordinate. Green curve presents generic richness. Magenta curve shows the proportion of non-nektonic animals. E, Early; L, Late; M, Middle; Chan, Changhsingian; Grie, Griesbachian; Di, Dienerian; S, Smithian; Sp, Spathian; Ani, Anisian; Ladi, Ladinian; Carn, Carnian; Rh, Rhaetian; Per, Permian.

non-motile, motile, and nektonic animals) (see Fig. 1). Non-motile or passive animals are either benthic or planktonic (*17*) and consist of epifaunal bivalves, brachiopods, bryozoans, hydrozoans, corals, pelmatazoan echinoderms, foraminifers, radiolarians, and sponges. Motile or active animals are defined as benthic animals with independent mobile ability (excluding free swimmers) and include annelids, infaunal bivalves, crustaceans, eleutherozoan echinoderms, gastropods, and scaphopods. Nekton are composed of cephalopods, conodonts, fishes, and marine reptiles.

The three functional groups exhibit different fates during and after the P-Tr extinction (Fig. 2C). The generic diversity of nekton suffered relatively little during the P-Tr extinction and increased gradually in the Early Triassic before reaching a peak in the early Anisian. Afterward, nekton diversity showed a continuous decline until the Rhaetian. Motile animals suffered severe losses during the P-Tr crisis, which resulted in a low Early Triassic diversity before a quick rebound in the initial Middle Triassic. Non-motile animals suffered the most severe extinction, and their diversity declined markedly from more than 500 genera in the Late Permian to fewer than 100 genera in the Early Triassic. Non-motile animals achieved pre-extinction levels after a rapid rebound in the initial Middle Triassic.

The faunal shift resulted in a change of ecosystem structure to one dominated by nektonic groups (Fig. 3). Our data provide information on genus richness and occurrence, not abundance, making it difficult to evaluate biomass for various ecological guilds. This problem is common to all fossil data studies; nonetheless, both taxon richness and occurrence information do have implications for predator-prey relationships (*18*). The proportion of nekton genera is around 14% in the Late Permian, but after mass extinction, it climbed rapidly and reached a peak (67%) in the Smithian, about 2 Ma later (Fig. 2E). Subsequently, it experienced a continued decline to 11% in the Rhaetian. The proportion of genera of non-motile animals exhibits a reverse trend to that of nekton: It declines from 71 to 21% throughout early Griesbachian to Smithian times, followed

Downloaded from http://advances.sciencemag.org/ on September 24, 2020

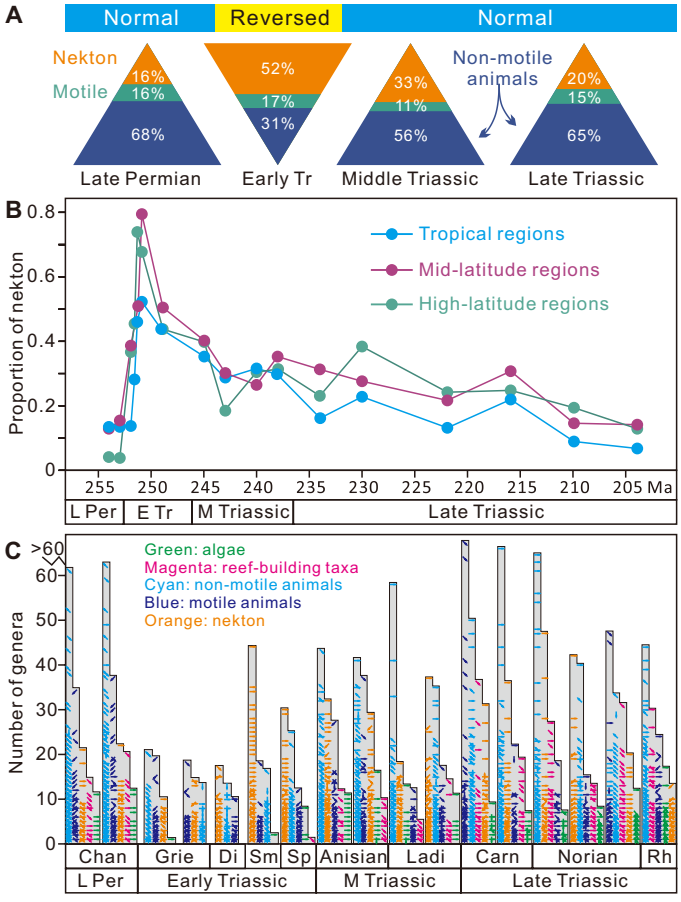

Fig. 3. Evolution of marine ecosystems throughout the Late Permian to Late Triassic. (**A**) Functional pyramids in generic diversity among non-motile, motile, and nektonic groups from four geological intervals, indicating a reversed pyramid in the Early Triassic. The size of proportions is represented by the area of the triangles. (**B**) Proportion of nekton in generic occurrences (see fig. S3 for subdivisions of latitudinal regions). (**C**) Generic richness for all marine communities (see details in fig. S4). A community is a collection of fossils from the same stratigraphic unit in a location. Each arrow shows the number of genera for a particular community. Green color shows algae including calcareous algae (3 o'clock arrow), dinoflagellates (5 o'clock arrow), and coccoliths (6 o'clock arrow). Magenta color shows reef-building animals including corals (3 o'clock arrow) and sponges (5 o'clock). Cyan color shows non-motile animals including hydrozoans (1 o'clock arrow), radiolarians (3 o'clock arrow), brachiopods (5 o'clock arrow), epifaunal bivalves (6 o'clock arrow), bryozoans (7 o'clock arrow), pelmatazoan echinoderms (9 o'clock arrow), and foraminifers (11 o'clock arrow). Blue color shows motile animals including infaunal bivalves (3 o'clock arrow), gastropods (5 o'clock arrow), eleutherozoan echinoderms (6 o'clock arrow), and ostracods (7 o'clock arrow). Orange color shows nekton including cephalopods (3 o'clock arrow), conodonts (5 o'clock arrow), fishes (7 o'clock arrow), and marine reptile (12 o'clock arrow).

by a long-term increase and final return to 70% in the Rhaetian. In contrast, the proportion of generic occurrences of motile animals shows little change at ~15% from Late Permian to Late Triassic times. The proportion of generic richness among three groups shows a trend similar to that of occurrence data but with smaller amplitude (Fig. 2C).

Data from different paleolatitudinal regions (see Fig. 3B) show that the trends in the composition and structure of marine ecosystems are independent of latitude: The proportion of nekton in tropical, middle-latitude, and high-latitude regions shows a similar trend throughout the Late Permian to Late Triassic (Fig. 3B). All three curves exhibit plateaus in the middle Early Triassic. Higher-latitude regions show a relatively higher proportion, and the peak value of nekton is more than 70% in the middle- and high-latitude regions. This pattern may be the result of poleward migration of nekton because tropical ecosystems had a higher risk of extinction as sea surface temperature may have reached 40°C at this time (*14*). All three curves exhibit moderately decreasing trends in a moderate manner throughout the Smithian to Rhaetian.

Reversed functional pyramid in Early Triassic oceans

The P-Tr mass extinction leads to a reversed functional pyramid for Early Triassic marine ecosystems, which are typically dominated by non-motile animals during both the Late Permian and the Middle-Late Triassic (Fig. 3A). The proportion of generic diversity comprising non-motile animals is 68% in the Late Permian Changhsingian (Fig. 3A), which is almost the same value seen in the Early and Middle Permian (*17*). This finding suggests that the marine ecosystem structure was not significantly changed during the end-Guadalupian extinction event. Exceptionally, the Early Triassic saw nekton dominate the functional pyramid of this time. Rarefaction analysis shows that the reversed functional pyramid is not an artifact of sampling (Fig. 2C and fig. S2). The reversed pyramid is a result of both a major decrease of non-motile diversity and an increase of nekton diversity (Fig. 2C). Both intrinsic (biotic) and extrinsic (abiotic) factors may have been responsible for this faunal turnover. Potentially, nekton have a wider fundamental niche than benthos and plankton because of their free-moving ability. In addition, non-nektonic animals suffered more severely during the P-Tr mass extinction and their recovery was sluggish, coinciding with a prolongation of harmful conditions in benthic environments (*15*). The fundamental niche of nekton also shrank during the crisis, as testified by their extinction losses, but their realized niches probably expanded because of the relaxation of competition stress (*19*). Therefore, the turnover between nekton and non-motile animals reflects the ecosystem succession from a normal one under stable environments to an abnormal one under environmental perturbations that were at their most severe in the benthic realm.

The reversed functional pyramid has profound implications for the energy flow in marine ecosystems of the Early Triassic. Nekton such as cephalopods (all), conodonts (most), fishes (most), and marine reptiles (all) usually occupy the top trophic levels as predators (*18*). The rapid diversification of predators implies that Early Triassic simple marine ecosystems probably had simple food webs and short food chains. There are at least two good reasons to support this inference. First, the maximum genus richness for all communities except for nekton decreased markedly in the Early Triassic (Fig. 3C), which would have resulted in a significant drop in the number of links for the food web because of the positive correlation between links of the food web and biodiversity in a community (*20*). For nekton, the maximum generic richness decreased moderately in the Griesbachian and Dienerian but rebounded to much higher levels in the Smithian and Spathian (Fig. 3C). Second, the expanded proportion of predators requires more energy flow to the top trophic level and shortening the length of the food chain achieves this (*21*). The apparent vulnerable nature of the ecosystem at this time is also supported by the dominance of opportunistic organisms in the aftermath of the P-Tr extinction (e.g., cyanobacteria, small foraminifers, *Claraia* bivalves, and linguloid brachiopods) (*2*, *22*).

Downloaded from http://advances.sciencemag.org/ on September 24, 2020

Decoupling of taxonomic and ecological recoveries

Our study shows that the recovery of global marine ecosystems from macroecological disturbance is decoupled from taxonomic recovery. The evolutionary recovery is judged by the stable global taxonomic diversity seen from the early Anisian onward. In comparison, global ecosystem restoration, represented by the gradual decrease in proportion of nekton after the Smithian and the continued increase in richness of metazoan reefs, was still ongoing in the latest Triassic (Rhaetian), ~50 Ma later, when the next mass extinction struck at the end-Triassic (*23*). Restoration of marine ecosystems is characterized by a gradual increase in complexity and stability (as seen in the accelerated increase of community diversity in the Smithian, Spathian, and Anisian), the appearance of large top predators (marine reptiles) in the Spathian, and the emergence of coral-sponge reefs and new phytoplankton groups (e.g., coccoliths and dinoflagellates) in the Middle Triassic that became diverse and widespread in the Late Triassic [Fig. 3C; see also the study of Kiessling (*24*)].

While there is a logistic increase in generic richness (Fig. 2, B and F), the increase in the proportion of non-nektonic animals during ecosystem restoration occurs in an explicitly logarithmic manner ($R = 0.99$, $P \ll 0.001$; Fig. 2, D and F). The logarithmic increase suggests that the speed of reestablishment of ecological structure was in gradual decline. The initial period of rapid increase is primarily caused by a rapid increase in diversity of non-motile and motile animals' diversity in the Smithian, Spathian, and early Anisian (Fig. 2C). The latter period of slow change reflects a slow and prolonged decrease in nekton diversity, combined with the facts that benthic diversity remained stable (Fig. 2C), and diversity of reef-building communities increased only incrementally (Fig. 3C). This trend persisted until the end of the Triassic when the proportion of nekton had declined to a level last seen in the latest Permian. It is important to be aware of this trend when evaluating the nature and timing of the end-Triassic mass extinction. It has been frequently noted that marine taxonomic diversity was in decline, especially among ammonoids (*9*), in the last few million years of the Triassic and that the mass extinction was little more than a coup de grace, thus questioning the status of this crisis as one of the "big five" (*25*). This view fails to appreciate the long-term trend of ecosystem evolution throughout the Middle-Late Triassic. Nekton decline had been underway since the beginning of the Middle Triassic, but it was not matched by a decline in benthic groups that maintained their diversity until the end of the Triassic (Fig. 2C). The end-Triassic mass extinction is therefore best viewed as an abrupt termination of a ~50-Ma trend.

Our data show a decline in both raw and subsampled diversity in the middle Carnian (Fig. 2A). All three groups (i.e., non-motile, motile, and nektonic animals) were obviously affected by this event (Fig. 2C). The decline of generic richness in the middle Carnian is not shown in earlier biodiversity curves (*1*, *3*). This trend can probably be explained by the fact that this event falls within a traditional time bin and thus is masked, although an extinction peak for ammonoids and echinoderms has been seen in the middle Carnian (*26*, *27*). However, the middle Carnian extinction event did not significantly affect the increase in proportion of non-nektonic animals (Fig. 2D), suggesting that this event had little long-term impact on the ecological structure of marine ecosystems. This inference is supported by the recent finding that environmental perturbations associated with the Carnian Pluvial Event such as climatic warming and oceanic anoxia were not so severe compared to the P-Tr event (*14*, *15*, *28*).

The stepwise recovery hypothesis has favored ecosystem rebuilding in a stepwise manner from bottom to top trophic levels in the Early Triassic (*8*). However, our quantitative analysis suggests a bottom-to-top destruction for marine ecosystems followed by ecosystem restoration in a top-to-bottom order. The selective extinction of non-motile primary consumers during the P-Tr event (*29*), followed by their suppressed recovery, ensured that non-motile animals were the biggest victims in Early Triassic oceans. In contrast, high-level predators including cephalopods, conodonts, and fishes diversified and become the most diverse fauna at this time. Therefore, marine ecosystems collapsed in an explicitly bottom-to-top manner. The ecosystem rebuilding is characterized by diversity increase of lower-level consumers.

In summary, our data reveal that the restoration of marine ecosystem structure (~50 Ma) was an order of magnitude slower than rates of taxonomic diversity recovery (~5 Ma). The decoupling of taxonomic and ecological recoveries reflects distinctive drivers: (i) The close link between the rapid rebound in taxonomic richness and the environmental amelioration in the initial Middle Triassic indicates that environmental carrying capacity plays a critical role in controlling taxonomic diversity, and (ii) the prolonged recovery in ecosystem structure likely reflects the complex interactions in ecosystems (e.g., interactions among species within clades, interactions between clades, and interactions between biotic and abiotic factors) that saw logarithmic rates of change. In contrast, the logistic growth of taxonomic diversity suggests a process of vacant niche filling that was independent of ecosystem structure. This study reaffirms the importance of protecting global ecosystem diversity because, once it is destroyed, restoration requires dozens of million years, much longer than human history.

MATERIALS AND METHODS

Database

To analyze the nature of the P-Tr mass extinction and recovery in the Triassic, marine fossil occurrences were collected from the Late Permian (Changhsingian, 254.1 Ma ago) to the Late Triassic (Rhaetian, 201.3 Ma ago). Taphonomic, stratigraphic, and geographic data were recorded for fossil collections. Like most paleontological databases, we compiled occurrences at the generic level as species determination is often inaccurate and patchy and the inclusion of indeterminate species occurrences is vital for boosting sample sizes. A total of 51,055 occurrences derived from 4221 collections in 1679 literature sources were collected and assigned to time bins at substage- or stage-level resolution. The total number of genera is 4321, which belong to 20 major marine groups (i.e., calcareous algae, coccoliths, dinoflagellates, corals, sponges, brachiopods, bryozoans, echinoderms, foraminifers, bivalves, radiolarians, hydrozoans, gastropods, annelids, ostracods, non-ostracod crustaceans, cephalopods, conodonts, fishes, and marine reptiles).

We binned the collection data into a series of 17 substage- or stage-level time intervals, averaging 3.1 Ma in duration. Subdivisions are primarily based on biostratigraphic data (see details in table S1) as well as chemostratigraphic data when available. These bins are, in sequential order, early Changhsingian, late Changhsingian, early Griesbachian, late Griesbachian, Dienerian, Smithian, Spathian, early Anisian, late Anisian, early Ladinian, late Ladinian, early Carnian, late Carnian, early Norian, middle Norian, late Norian, and Rhaetian.

Downloaded from http://advances.sciencemag.org/ on September 24, 2020

Only occurrences with explicit generic assignments were included in our fossil database. The sifting criteria were as follows: (i) Indeterminate, unnamed, and misspelled taxa were excluded; (ii) ichnofossils were excluded; (iii) non-marine collections were excluded; (iv) multiple occurrences of the same genus in a single collection were treated as a single occurrence; (v) collections with uncertain stratigraphic ranges were excluded; and (vi) subgenera were treated as separate genera.

Subsampling method

We used classic rarefaction to equalize sample sizes across our time bins. Rarefaction seeks to draw a fixed number of specimens per time interval, either directly or by adopting a proxy based on numbers of taxa occurrences or fossil collections (*30*, *31*). Here, we used counts of generic occurrences as the proxy because our database includes both protozoan and metazoan fossil groups that have great differences in counts of specimens for each collection. Protozoan groups such as foraminifer and radiolarian with their small body sizes (<1 mm) generally have a much larger number of specimens compared to metazoan groups like bivalves, brachiopods, ammonoids, and fishes with their larger body sizes. In addition, fragmentary fossils (i.e., crinoid ossicles) would count as a single specimen but could have come from the same organism.

Rarefaction curves for all 17 time bins are presented in fig. S1. Direct comparisons of the Late Permian and Early, Middle, and Late Triassic curves suggest that the lower diversity of Early Triassic bins is not an artifact of sample size. In contrast to the raw data, when the late Changhsingian sample is rarefied to the size of the early Changhsingian sample, they exhibit little difference in genus richness. Similarly, for Middle Triassic bins, when the Anisian sample is rarefied to the size of the Ladinian sample, they exhibit similar genus richness. However, the significantly greater value of genus richness found in the early Carnian raw data is still seen when the sample is rarefied to the size of the nearby sample.

Rarefaction curves for non-motile, motile, and swimming groups in the late Changhsingian, Griesbachian, Dienerian, Smithian, Spathian, early Anisian, early Carnian, and Rhaetian are presented in fig. S2. Direct comparisons of these curves suggest that the reversed functional pyramid for Early Triassic marine ecosystems is not an artifact of sample size. For Late Permian and Middle and Late Triassic bins, when the samples of the three different groups are rarefied to the same size, non-motile animals always have the highest genus richness. However, for the Early Triassic bins (see Dienerian, Smithian, and Spathian), when the samples of the three groups are rarefied to the same size, swimming animals have the highest genus richness. In Fig. 2 (A and C), we rarefied to $n = 1400$ for the entire data set and then $n = 510$, 184, and 330 for non-motile, motile, and swimming groups, respectively.

Paleolatitude analysis

Paleolatitude data were obtained using PointTracker v7 rotation files applied to modern latitude and longitude data. Many bins are the same as they are in 10-Ma intervals (e.g., 250 Ma including early Changhsingian, late Changhsingian, early Griesbachian, late Griesbachian, Dienerian, Smithian, Spathian, and early Anisian; 240 Ma including late Anisian, early Ladinian, and late Ladinian; 230 Ma including early and late Carnian; 220 Ma including early and middle Norian; 210 Ma including late Norian and Rhaetian). Fossil collections were assigned into three bins with different paleolatitudes (i.e., tropical regions with paleolatitudes between 23.5°N and 23.5°S; middle-latitude regions with paleolatitudes between 23.5°N and 40°S in both northern and southern hemispheres, respectively; and high-latitude regions with paleolatitudes between 40°N and 90°S in both northern and southern hemispheres, respectively). The division is based on modern sea surface temperature because large temperature gradients occur in these three regions (see fig. S3). For modern oceans, sea surface temperature is generally more than 25°C, between 15° and 25°C, and less than 15°C in low-, middle-, and high-latitude regions, respectively.

SUPPLEMENTARY MATERIALS

Supplementary material for this article is available at http://advances.sciencemag.org/cgi/content/full/4/10/eaat5091/DC1

Fig. S1. Comparative rarefaction curves for the 17 time bins based on analysis of our global database of genus occurrences.

Fig. S2. Comparative rarefaction curves for non-motile, motile, and swimming animals in the late Changhsingian, Griesbachian, Dienerian, Smithian, Spathian, early Anisian, early Carnian, and Rhaetian.

Fig. S3. Annual mean sea surface temperature (1971–2000).

Fig. S4. Generic richness of marine communities.

Table S1. Conodont and ammonoid stratigraphic data for the Triassic fossil database.

External Database S1. Late P-Tr biotic data.

References (*32*–*38*)

REFERENCES AND NOTES

1. J. J. Sepkoski Jr., A kinetic model of Phanerozoic taxonomic diversity, III. Post-Paleozoic families and mass extinctions. *Paleobiology* **10**, 246–267 (1984).
2. A. Hallam, P. B. Wignall, *Mass Extinctions and Their Aftermath* (Oxford Univ. Press, 1997).
3. J. Alroy, M. Aberhan, D. J. Bottjer, M. Foote, F. T. Fürsich, P. J. Harries, A. J. Hendy, S. M. Holland, L. C. Ivany, W. Kiessling, M. A. Kosnik, C. R. Marshall, A. J. McGowan, A. I. Miller, T. D. Olszewski, M. E. Patzkowsky, S. E. Peters, L. Villier, P. J. Wagner, N. Bonuso, P. S. Borkow, B. Brenneis, M. E. Clapham, L. M. Fall, C. A. Ferguson, V. L. Hanson, A. Z. Krug, K. M. Layou, E. H. Leckey, S. Nürnberg, C. M. Powers, J. A. Sessa, C. Simpson, A. Tomasovych, C. C. Visaggi, Phanerozoic trends in the global diversity of marine invertebrates. *Science* **321**, 97–100 (2008).
4. S.-z. Shen, J. L. Crowley, Y. Wang, S. A. Bowring, D. H. Erwin, P. M. Sadler, C.-q. Cao, D. H. Rothman, C. M. Henderson, J. Ramezani, H. Zhang, Y. Shen, X.-d. Wang, W. Wang, L. Mu, W.-z. Li, Y.-g. Tang, X.-l. Liu, L.-j. Liu, Y. Zeng, Y.-f. Jiang, Y.-g. Jin, Calibrating the end-Permian mass extinction. *Science* **334**, 1367–1372 (2011).
5. S. M. Stanley, Estimates of the magnitudes of major marine mass extinctions in earth history. *Proc. Natl. Acad. Sci. U.S.A.* **113**, E6325–E6334 (2016).
6. P. D. Roopnarine, K. D. Angielczyk, Community stability and selective extinction during the Permian-Triassic mass extinction. *Science* **350**, 90–93 (2015).
7. D. H. Erwin, The end and the beginning: Recoveries from mass extinction. *Trends Ecol. Evol.* **13**, 344–349 (1998).
8. Z.-Q. Chen, M. J. Benton, The timing and pattern of biotic recovery following the end-Permian mass extinction. *Nat. Geosci.* **5**, 375–383 (2012).
9. A. Brayard, G. Escarguel, H. Bucher, C. Monnet, T. Brühwiler, N. Goudemand, T. Galfetti, J. Guex, Good genes and good luck: Ammonoid diversity and the end-Permian mass extinction. *Science* **325**, 1118–1121 (2009).
10. S. M. Stanley, Evidence from ammonoids and conodonts for multiple Early Triassic mass extinctions. *Proc. Natl. Acad. Sci. U.S.A.* **106**, 15264–15267 (2009).
11. C. Romano, M. B. Koot, I. Kogan, A. Brayard, A. V. Minikh, W. Brinkmann, H. Bucher, J. Kriwet, Permian–Triassic Osteichthyes (bony fishes): Diversity dynamics and body size evolution. *Biol. Rev.* **91**, 106–147 (2016).
12. W. J. Foster, R. J. Twitchett, Functional diversity of marine ecosystems after the Late Permian mass extinction event. *Nat. Geosci.* **7**, 233–238 (2014).
13. A. Ruffell, M. J. Simms, P. B. Wignall, The carnian humid episode of the late Triassic: A review. *Geol. Mag.* **153**, 271–284 (2016).
14. Y. Sun, M. M. Joachimski, P. B. Wignall, C. Yan, Y. Chen, H. Jiang, L. Wang, X. Lai, Lethally hot temperatures during the Early Triassic greenhouse. *Science* **338**, 366–370 (2012).
15. K. V. Lau, K. Maher, D. Altiner, B. M. Kelley, L. R. Kump, D. J. Lehrmann, J. C. Silva-Tamayo, K. L. Weaver, M. Yu, J. L. Payne, Marine anoxia and delayed Earth system recovery after the end-Permian extinction. *Proc. Natl. Acad. Sci. U.S.A.* **113**, 2360–2365 (2016).
16. M. Aberhan, W. Kiessling, Phanerozoic marine biodiversity: A fresh look at data, methods, patterns and processes, in *Earth and Life*, J. A. Talent, Ed. (Springer, 2012), pp. 3–22.

Downloaded from http://advances.sciencemag.org/ on September 24, 2020

17. R. K. Bambach, A. H. Knoll, J. J. Sepkoski Jr., Anatomical and ecological constraints on Phanerozoic animal diversity in the marine realm. *Proc. Natl. Acad. Sci. U.S.A.* **99**, 6854–6859 (2002).
18. M. Kowalewski, P. H. Kelley, P. Dodson, R. K. Bambach, Supporting predators: Changes in the global ecosystem inferred from changes in predator diversity, in *The Fossil Record of Predation*, M. Kowalewski, P. H. Kelley, P. Dodson, Eds. (The Paleontological Society, 2002), vol. 8, pp. 319–352.
19. A. J. McGowan, Ammonoid taxonomic and morphologic recovery patterns after the Permian-Triassic. *Geology* **32**, 665–668 (2004).
20. P. D. Roopnarine, Networks, extinction, and palecommunity food webs, in *Quantitative Methods in Paleobiology*, J. Alroy, G. Hunt, Eds. (The Paleontological Society, 2010), vol. 16, pp. 143–161.
21. E. M. Dickman, J. M. Newell, M. J. González, M. J. Vanni, Light, nutrients, and food-chain length constrain planktonic energy transfer efficiency across multiple trophic levels. *Proc. Natl. Acad. Sci. U.S.A.* **105**, 18408–18412 (2008).
22. S. B. Pruss, D. J. Bottjer, F. A. Corsetti, A. Baud, A global marine sedimentary response to the end-Permian mass extinction: Examples from southern Turkey and the western United States. *Earth Sci. Rev.* **78**, 193–206 (2006).
23. A. M. Dunhill, W. J. Foster, J. Sciberras, R. J. Twitchett, Impact of the Late Triassic mass extinction on functional diversity and composition of marine ecosystems. *Palaeontology* **61**, 133–148 (2018).
24. W. Kiessling, Reef expansion during the Triassic: Spread of photosymbiosis balancing climatic cooling. *Palaeogeogr. Palaeoclimatol. Palaeoecol.* **290**, 11–19 (2010).
25. A. Hallam, How catastrophic was the end-Triassic mass extinction? *Lethaia* **35**, 147–157 (2002).
26. M. J. Benton, More than one event in the late Triassic mass extinction. *Nature* **321**, 857–861 (1986).
27. M. J. Simms, A. H. Ruffell, Synchroneity of climatic change and extinctions in the Late Triassic. *Geology* **17**, 265–268 (1989).
28. Y. D. Sun, P. B. Wignall, M. M. Joachimski, D. P. G. Bond, S. E. Grasby, X. L. Lai, L. N. Wang, Z. T. Zhang, S. Sun, Climate warming, euxinia and carbon isotope perturbations during the Carnian (Triassic) Crisis in South China. *Earth Planet. Sci. Lett.* **444**, 88–100 (2016).
29. H. Song, P. B. Wignall, J. Tong, H. Yin, Two pulses of extinction during the Permian-Triassic crisis. *Nat. Geosci.* **6**, 52–56 (2013).
30. A. I. Miller, M. Foote, Calibrating the Ordovician radiation of marine life: Implications for Phanerozoic diversity trends. *Paleobiology* **22**, 304–309 (1996).
31. J. Alroy, C. Marshall, R. Bambach, K. Bezusko, M. Foote, F. Fürsich, T. Hansen, S. Holland, L. Ivany, D. Jablonski, D. K. Jacobs, D. C. Jones, M. A. Kosnik, S. Lidgard, S. Low, A. I. Miller, P. M. Novack-Gottshall, T. D. Olszewski, M. E. Patzkowsky, D. M. Raup, K. Roy, J. J. Sepkoski Jr., M. G. Sommers, P. J. Wagner, A. Webber, Effects of sampling standardization on estimates of Phanerozoic marine diversification. *Proc. Natl. Acad. Sci. U.S.A.* **98**, 6261–6266 (2001).
32. National Oceanic and Atmospheric Administration, Annual mean sea surface temperature: 1971–2000; www.cpc.ncep.noaa.gov/products/precip/realtime/clim/annual/monthly/annual.sst.html
33. N. R. Ainsworth, W. Braham, F. J. Gregory, B. Johnson, C. King, A proposed latest Triassic to earliest Cretaceous microfossil biozonation for the English Channel and its adjacent areas. *Geol. Soc. Spec. Publ.* **133**, 87–102 (1998).
34. S.-Z. Shen, S.-L. Mei, Lopingian (Late Permian) high-resolution conodont biostratigraphy in Iran with comparison to South China zonation. *Geol. J.* **45**, 135–161 (2010).
35. M. Balini, S. G. Lucas, J. F. Jenks, J. A. Spielmann, Triassic ammonoid biostratigraphy: An overview. *Geol. Soc. Spec. Publ.* **334**, 221–262 (2010).
36. F. M. Gradstein, J. G. Ogg, M. Schmitz, G. Ogg, *The Geologic Time Scale 2012* (Elsevier, 2012).
37. J. F. Jenks, C. Monnet, M. Balini, A. Brayard, M. Meier, Biostratigraphy of Triassic ammonoids, in *Ammonoid Paleobiology: From Macroevolution to Paleogeography*, C. Klug, D. Korn, K.D. Baets, I. Kruta, R.H. Mapes Eds. (Springer, 2015), pp. 329–388.
38. J. G. Ogg, G. Ogg, F. M. Gradstein, *A Concise Geologic Time Scale: 2016* (Elsevier, 2016).

Acknowledgments: We thank J. Chen, Y. Huang, X. Dai, and R. Bai for providing useful comments on the fossil database. We thank the contributors to the Paleobiology Database. This is Paleobiology Database publication number 321. **Funding:** H.S. was supported by the State Key R&D Project of China (2016YFA0601100), Strategic Priority Research Program of Chinese Academy of Sciences (XDB26000000), the National Natural Science Foundation of China (41622207, 41530104, 41821001, and 41661134047), and a Marie Curie Fellowship (H2020-MSCA-IF-2015-701652). P.B.W. was funded by the Natural Environment Research Council (grant NE/P0137224/1), part of the Biosphere Evolution, Transitions and Resilience (BETR) programme. A.M.D. was funded by a Leverhulme Early Career Fellowship (ECF-2015-044). **Author contributions:** H.S. and P.B.W. conceived the research and wrote the paper. A.M.D. contributed to the discussion. **Competing interests:** The authors declare that they have no competing interests. **Data and materials availability:** All data needed to evaluate the conclusions in the paper are present in the paper and/or the Supplementary Materials. Additional data related to this paper may be requested from the authors.

Submitted 6 March 2018
Accepted 5 September 2018
Published 10 October 2018
10.1126/sciadv.aat5091

Citation: H. Song, P. B. Wignall, A. M. Dunhill, Decoupled taxonomic and ecological recoveries from the Permo-Triassic extinction. *Sci. Adv.* **4**, eaat5091 (2018).

Downloaded from http://advances.sciencemag.org/ on September 24, 2020

Science Advances

Decoupled taxonomic and ecological recoveries from the Permo-Triassic extinction

Haijun Song, Paul B. Wignall and Alexander M. Dunhill

Sci Adv **4** (10), eaat5091.
DOI: 10.1126/sciadv.aat5091

ARTICLE TOOLS http://advances.sciencemag.org/content/4/10/eaat5091

SUPPLEMENTARY MATERIALS http://advances.sciencemag.org/content/suppl/2018/10/05/4.10.eaat5091.DC1

REFERENCES This article cites 30 articles, 18 of which you can access for free
http://advances.sciencemag.org/content/4/10/eaat5091#BIBL

PERMISSIONS http://www.sciencemag.org/help/reprints-and-permissions

Use of this article is subject to the Terms of Service

Science Advances (ISSN 2375-2548) is published by the American Association for the Advancement of Science, 1200 New York Avenue NW, Washington, DC 20005. The title *Science Advances* is a registered trademark of AAAS.

Copyright © 2018 The Authors, some rights reserved; exclusive licensee American Association for the Advancement of Science. No claim to original U.S. Government Works. Distributed under a Creative Commons Attribution NonCommercial License 4.0 (CC BY-NC).

Downloaded from http://advances.sciencemag.org/ on September 24, 2020